SPICE Modeling of Free-Space Optical Systems

Ahmed Hussein[*]

MEMScAP, Inc.

aosman@ieee.org

Ahmed Nounou

SoftMEMS, LLC

ahmed.nounou@softmems.com

Nehal Saada[†]

SoftMEMS, LLC

nehal.saada@gmail.com

Dina Atef

SoftMEMS, LLC

dina.atef@softmems.com

Diaa Khalil

Ain-Shams University

diaa.khalil@ieee.org

ABSTRACT

A three dimensional free-space optical library is developed and implemented using C language inside a SPICE simulator for accurate and realistic co-simulation with electronic and electromechanical elements. A parametric, transient, and Monte-Carlo simulation of a 2x2 optical switch is demonstrated using this library.

1. INTRODUCTION

The interdisciplinary nature of Micro-Electro-Mechanical Systems (MEMS) is a significant bottleneck in the timely design of new products incorporating MEMS technology. Design tools are needed to combine aspects of EDA (Electronic Design Automation) with mechanical, thermal, fluidic, optical, and magnetic simulation tools. These design tools should also allow for both top-down design as well as bottom-up verification approaches [1]. The problem is more pronounced with Optical MEMS components where the simulator should deal with the spatial variation of the signal as well as its propagating nature. In this paper, we demonstrate how to use the SPICE environment in MEMS Pro[TM] together with the proposed optical library in the design of a MEMS-based 2x2 optical switch [2]. Both the static and dynamic behaviors of the switch have been considered. In addition, a Monte-Carlo simulation of the switch insertion loss is done for the purpose of yield analysis.

SPICE simulation is widely known in the field of electronics. The kernel of any SPICE simulator is a matrix solver that uses techniques like Newton-Raphson to find the solution of the *"across"* quantity (voltage) at each node and the *"through"* quantity (current) at each branch. Convergence is reached when Kirchoff's Voltage Law holds for all loops and Kirchoff's Current Law holds at every node [3]. The powerful SPICE solver can be utilized as well to solve other problems in other disciplines, for example, mechanical, thermal, fluidic, and optical domains by redefining the *across* and *through* quantities. The interdisciplinary action is taken care of implicitly inside the definition of these quantities. This concept is known as *"macromodeling"*.

---

*Ahmed Hussein is currently with Ain-Shams University
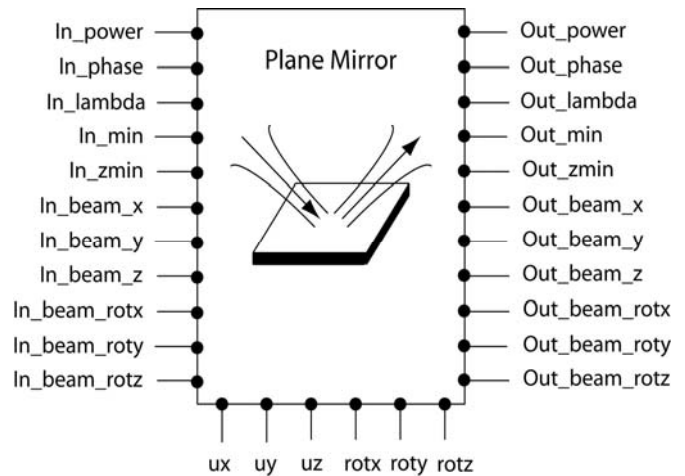†Nehal Saada is currently with Mentor Graphics, Egypt

Figure 1 Plane Mirror Schematic Symbol

Another technique is the usage of hardware description languages with mixed signal capabilities like HDL-A, VHDL-AMS, or Verilog A. Although more flexible and easier to implement, this technique is relatively slower when compared to compiled C language behavioral models implemented directly as dynamic linked libraries that the SPICE simulator may seamlessly call, especially for large components count. Besides, HDL compilers and interpreters with mixed-signal support are not as widespread as SPICE simulators that support C language user-defined models.

2. BASIC THEORY

The output of single-mode fibers or laser sources can be approximated, to the first-order, by a gaussian beam [4]. Fortunately, many free-space optical components, like mirrors, lenses, beam splitters, etc. will not affect much the validity of this approximation. A gaussian beam travelling along the $z-$axis can be represented mathematically as

$$E\left(\rho\right)=A\,\frac{\omega_0}{\omega(z)}\exp\left[-\frac{\rho^2}{\omega^2(z)}\right]\exp\left[-jkz-jk\,\frac{\rho^2}{2R(z)}+j\,\tan^{-1}\left(\frac{z}{z_0}\right)\right](1)$$

where A is the complex amplitude of the electric field, ω_0 is the minimum beam waist where the phase is constant, $\omega(z)$ is the beam waist at some distance z, k is the wave number and equals $2\pi/\lambda$, $R(z)$ is the radius of curvature

of the wavefront at distance z , and z_0 is the Rayleigh distance defined as the distance where the beam has expanded to $\sqrt{2}\omega_0$.

From (1), it is clear that we can fully characterize a Gaussian beam through eleven parameters, namely, beam power, P , which is proportional to $|A|^2$, beam phase, ϕ , beam wavelength, λ , minimum beam waist, ω_0 , the Rayleigh distance, z_0 position of the minimum beam waist, **beam_x**, **beam_y**, **beam_z**, and the directional cosines of the direction of propagation, **beam_rotx**, **beam_roty**, and **beam_rotz**.

As the gaussian beam is the signal flowing from one component to another, eleven optical ports will be needed to model the input/output gaussian beam. For example, a plane mirror will have twenty two optical ports for the input and output gaussian beams.

To fully describe and simulate an optical MEMS system, the components should be allowed to freely move during operation by being connected to other electromechanical components, like comb drives, gap-closing actuators, etc., for this purpose, a component will have six mechanical ports; three translational **ux**, **uy**, and **uz**, and three rotational, **rotx**, **roty**, and **rotz**. Figure 1 shows the schematic symbol for the plane mirror component.

Beside the ports that implement signal flow from one component to another, each component has two types of parameters; specific parameters, like reflectivity, radius of curvature, and diameters for a spherical mirror, and general parameters, which are common for all components, these include **x0**, **y0**, and **z0** for initial position, **comp_rotx**, **comp_roty**, and **comp_rotz** for initial orientation. For example, All the elements implemented in this library, are linear with respect to wavelength, and thus for all the components we have

$$\lambda_{out} = \lambda_{in} \qquad (2)$$

For proper simulation, each component should be able to identify its position and orientation relative to a certain origin so as to properly interact with its input. Thus, coordinate transformation should be performed using a 4x4 matrix to account for rotations as well as translations as follows

$$\begin{bmatrix} x_1 \\ y_1 \\ z_1 \\ 1 \end{bmatrix} = T_2 * RotX * RotY * RotZ$$

$$* RotX_{comp} * RotY_{comp} * RotZ_{comp} \qquad (3)$$

$$* T_1 \begin{bmatrix} x_0 \\ y_0 \\ z_0 \\ 1 \end{bmatrix}$$
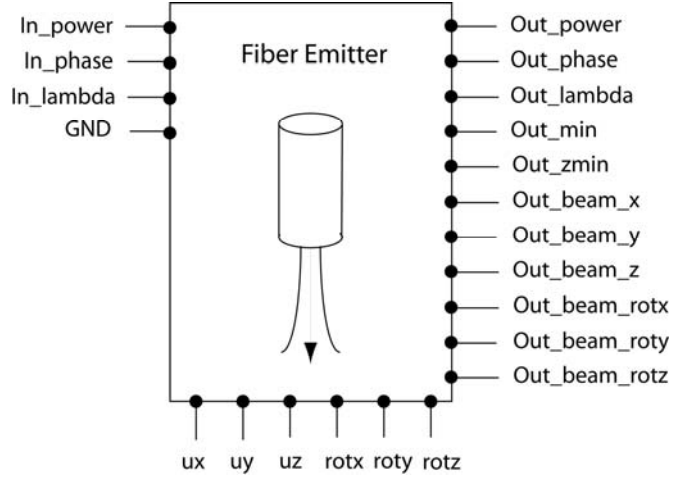

Figure 2 Fiber Emitter Schematic Symbol

where x_1 , y_1 , and z_1 are the coordinates of the component after transformation, x_0 , y_0 ,and z_0 are the initial coordinates of the component before transformation. $RotX$, $RotY$, and $RotZ$ are the rotational transformation matrices using the mechanical rotational ports **rotx**, **roty**, and **rotz** respectively. $RotX_{comp}$, $RotY_{comp}$, and $RotZ_{comp}$ are the initial orientation of the component around the origin. T_1 is a translational matrix used to temporarily transform the component to the origin to perform the rotation. T_2 is the final transformation of the component using the mechanical ports **ux**, **uy**, and **uz**. Now to calculate the new orientation of the component with motion, we find the transformation of the unit vector initially oriented on the z-axis, so we get

$$\begin{bmatrix} comp\_rotx1 \\ comp\_roty1 \\ comp\_rotz1 \\ 0 \end{bmatrix} = T_2 * RotX * RotY * RotZ$$

$$* RotX_{comp} * RotY_{comp} * RotZ_{comp} \qquad (4)$$

$$* T_1 \left(\begin{bmatrix} x_0 \\ y_0 \\ z_0 + 1 \\ 1 \end{bmatrix} - \begin{bmatrix} x_1 \\ y_1 \\ z_1 \\ 1 \end{bmatrix} \right)$$

For efficient computation, these equations are evaluated analytically and the coefficients that are function of the initial condition are evaluated once at instantiation of the model while the parts that are function of the ports are evaluated with time. We will now explain the modeling concept of three components that we will be using in 2x2 optical switch, namely the fiber emitter, the fiber receiver, and the plane mirror.
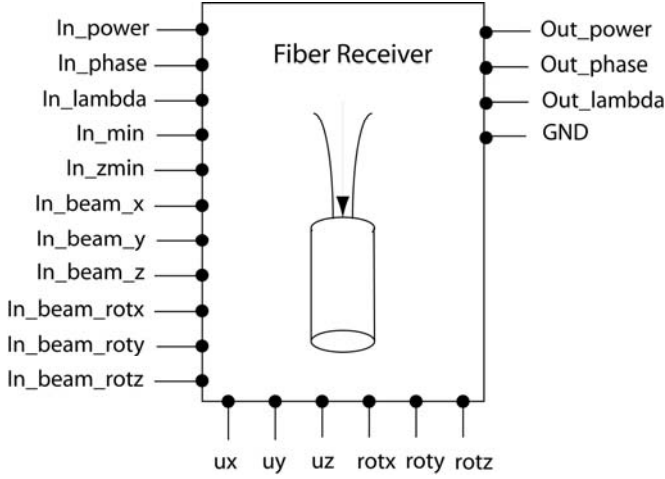
86

Figure 3 Fiber Receiver Schematic Symbol

The library demonstrated also includes three-dimensional spherical mirrors, thin lenses, sources, and detectors using the same modeling concept.

2.1 Fiber Emitter:

This model represents a single-mode fiber that emits Gaussian beam with the ports as shown in Figure 2. The model has also some specific parameters, core diameter, d_{core}, core refractive index, n_{core}, cladding refractive index, n_{clad}, end-face angle, efa.

2.2 Fiber Receiver:

This model represents a single-mode fiber that receives Gaussian beam with the ports. The specific parameters are defined in the same manner as the fiber emitter. Figure 3 shows the schematic symbol for the fiber receiver.

Through some mathematical manipulation, an analytical formula for three-dimensional coupling efficiency _ has been obtained. Thus, the output power is given as

$$P_{out} = \eta \left(beam\_x_{in/out}, beam\_y_{in/out}, beam\_z_{in/out}, \right.$$
$$\left. beam\_rotx_{in/out}, beam\_roty_{in/out}, beam\_rotz_{in/out} \right) P_{in} \quad (5)$$

2.3 Plane Mirror:

This model describes the reflection of a Gaussian beam from a plane surface. Figure 1 shows the schematic symbol of the plane mirror. Specific parameters for this model is the reflectivity.

To find the direction of the output gaussian beam knowing the input beam coordinates as well as the mirror position and orientation, we do the following vector analysis Let **v** be the vector representing the direction of propagation of the input beam, $\hat{\mathbf{n}}$ be a unit vector normal to the mirror, **w** be the vector in the direction of the output beam, then we have from Figure 4

$$\mathbf{v} + \mathbf{w} = 2\mathbf{v} + 2(\mathbf{v}.\hat{\mathbf{n}}) \quad (6)$$

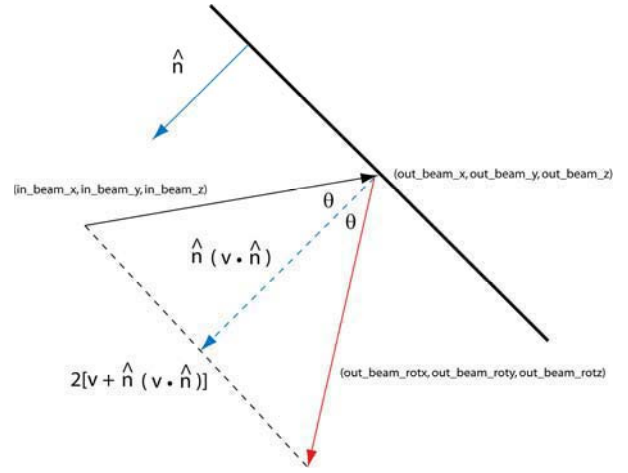From which we can directly calculate the direction of the output beam.

Figure 4 Vector Diagram for Plane Mirror

3. DESIGN DESCRIPTION

In our analysis, the free-space optical switch shown in Figure 5 is considered. This configuration has already been proposed in the literature and fabricated using DRIE technology [2].
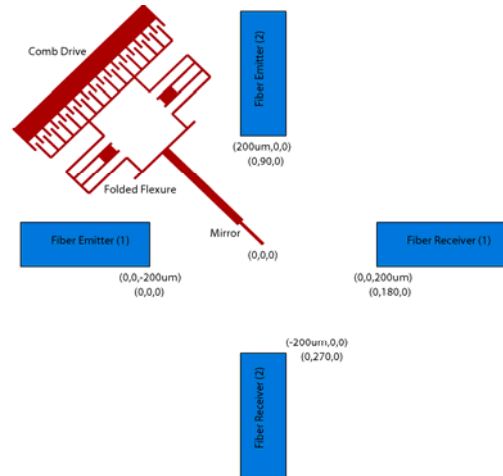

Figure 5 Schematic for a 2x2 Optical Switch

We will first construct the circuit with the schematic editor using a finite dimensions plane mirror, lensed fiber emitters, dual-input lensed fiber receivers, a comb drive actuator, a rigid plate, and a folded-flexure spring as shown in Figure 6.

87

The mirror used is a variant of the one represented in the previous section. It is considered as an element with two inputs and two outputs representing its two surfaces. Each input beam can either change direction due to reflection or propagate unaffected if not intercepted by the mirror. This is why the output from each surface is attached to two fiber receivers in Figure 6. Tables 1 and 2 represent the design parameters used for the various components.
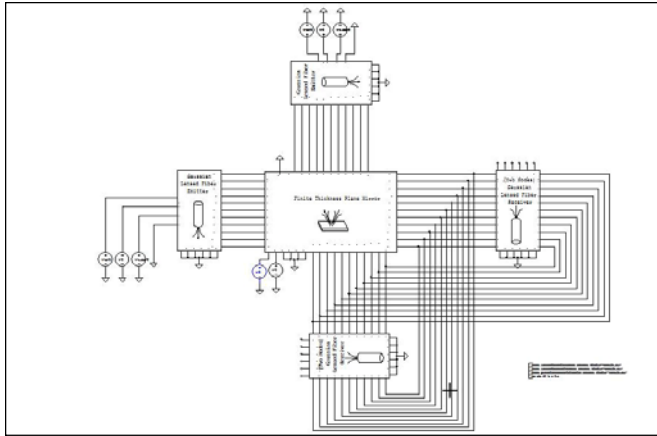

Figure 6 Circuit Schematic of the 2x2 Optical Switch

4. SIMULATION RESULTS

In this section, we present examples of the results showing the static and dynamic switch performance. Figure 7 and 8 show the effect of mirror thickness and fiber pointing error respectively on the switch insertion loss. It is clear that the mirror thickness effect introduces an additional lateral misalignment between the fibers whose effect decreases with increasing the beam waist. Figure 9 shows the dynamic behavior of the switch under pulsed input voltage applied on the comb drive.

The diagram shows the comb-drive displacement and the total power collected at fiber receiver 1. In order to illustrate the outputs from both sides of the mirror, the input power for fiber emitter 1 is half that of fiber emitter 2. The simulation took less than one minute on a Pentium 4, 1.6 GHz CPU and 256 MB RAM PC. Figure 10 is an example of a yield analysis using the built-in Monte Carlo simulation capabilities in SPICE simulators with 1000 samples [5]. The standard deviations of the optical parameters are given in Table 1.
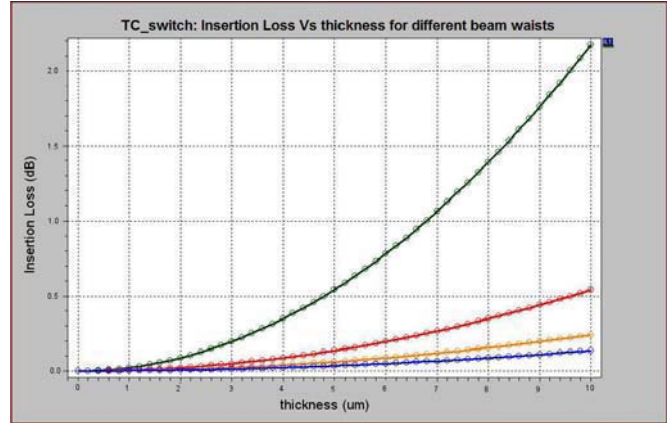

Figure 7 Insertion Loss Vs. Mirror Thickness (green, red, yellow, and blue) corresponds to w0=10,20,30, and 40 μm respectively
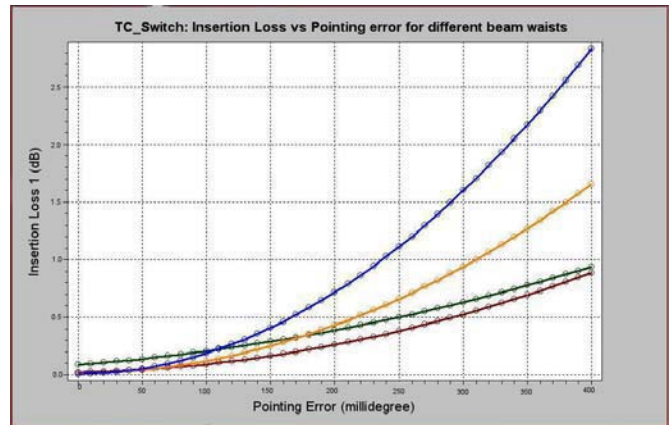

Figure 8 Insertion Loss Vs. Fiber Pointing Error (green, red, yellow, and blue) corresponds to w0=10,20,30, and 40 μm respectively

Table 1: Optical Design Parameters

Parameters	Nominal	Standard Deviation
Wavelength	1.55 μm	0 μm
Min. Beam Waiste	10 μm	5 μm
Fiber Working Distance Tx/Rx	400 μm	40 μm
Mirror Thickness	2 μm	0.5 μm
Fiber Pointing Error	0°	0.3°
Mirror Width	400 μm	0 μm
Mirror Height	80 μm	0 μm
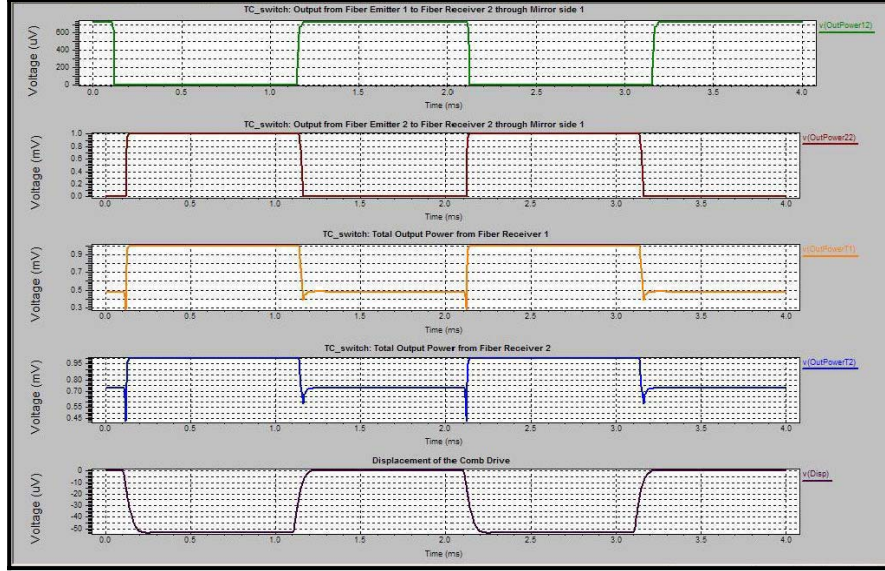
Figure 9 Timing Diagram

Table 2: Mechanical Design Parameters

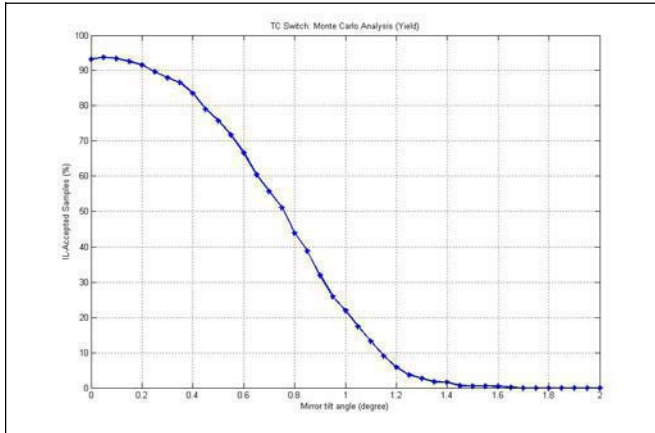| Parameters	Nominal
Number of Gaps	150
Gap Width	3 μm
Finger Length	300 μm
Initial Fingers Overlap	150 μm
Applied Voltage	15 V

Figure 10 Monte Carlo Results (Yield Analysis)

5. CONCLUSION

A 2x2 free-space optical MEMS switch is simulated using MEMS Pro™ to demonstrate the capabilities of the new three dimensional optical Gaussian library implemented in it. The simulation covers both the static and dynamic behavior of the switch. Also a Monte Carlo analysis using the built-in capabilities of already available SPICE simulators and schematic editors is applied to estimate the switch yield.

REFERENCES

[1] MEMS Pro:User's Manual, Release 5.1, SoftMEMS LLC, 2004.

[2] C. Marxer and N. F. de Rooij, "Micro-opto-mechanical 2x2 switch for single-mode fibers based on plasma-etched silicon mirror and electrostatic actuation," *J. Lightwave Technol.*, vol. 17, no. 1, pp. 2–6, Jan. 1999.

[3] R. M. Kielkowski, Ed., *Inside SPICE*. McGraw-Hill, Inc., 1998.

[4] W.B.Joyce and B.C. DeLoach, "Alignment of Gaussian beams," *Applied Optics*, vol. 23, no. 23, pp. 4187–4196, Dec. 1984.

[5] T. Badreldin, T. Saad, and D. Khalil, "Yield analysis of optical mems assembly process using a monte carlo simulation technique," *J. Lightwave Technol.*, vol. 23, no. 2, pp. 510–516, Feb. 2005.

APPENDIX

In this appendix, we derive the three-dimensional formula for power coupling efficiency between two misaligned Gaussian beams. Figure 11 shows the direction for the input Gaussian beam designated by $\langle in\_beam\_rotx, in\_beam\_roty, in\_beam\_rotz \rangle$ and the direction of the fiber receiver designated by $\overline{A} = \langle x_i, y_j, z_k \rangle$. The longitudinal offset between the two Gaussian beams can, thus, be given as

$$z_{off} = (x_1 - x_0)(in\_beam\_rotx) + (y_1 - y_0)(in\_beam\_roty) + (z_1 - z_0)(in\_beam\_rotz) \tag{7}$$
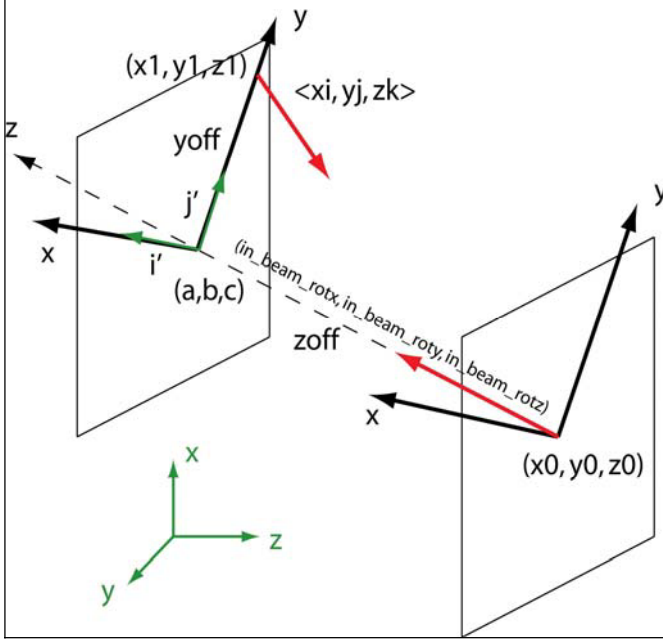
89

Figure 11 Coupling Efficiency Derivation

Let (a,b,c) be a point on the optical axis of the input Gaussian beam and lie on the same normal plane with the center of the fiber receiver, as shown in Figure 11. Then the lateral offset y_{off} is given by

$$y_{off} = \sqrt{(a-x_1)^2 + (b-y_1)^2 + (c-z_1)^2} \qquad (8)$$

We deliberately choose to let all the lateral offset in the $y'-$ direction. To calculate the angular misalignment between the two Gaussian beams, we define the two angles θ_x and θ_y as the angle between the input Gaussian beam and the projection of the fiber receiver's optical axis on the $yz-$ and $xz-$planes respectively, and is given by

$$\theta_x = \cos^{-1}\left[\frac{(\overline{A} \perp \hat{i}')\cdot\langle in\_beam\_rotx, in\_beam\_roty, in\_beam\_rotz\rangle}{\|(\overline{A} \perp \hat{i}')\|}\right]$$

$$\theta_y = \cos^{-1}\left[\frac{(\overline{A} \perp \hat{j}')\cdot\langle in\_beam\_rotx, in\_beam\_roty, in\_beam\_rotz\rangle}{\|(\overline{A} \perp \hat{j}')\|}\right] \quad (9)$$

Now we evaluate the overlap integral between the two Gaussian beams representing the power coupling coefficients, η as follows

$$\eta = \frac{2}{\pi|E_{in}|^2\,\omega_{in}^2}\int_{-\infty}^{\infty}\int_{-\infty}^{\infty}E_{in}(x,y,z)\big|_{z'=0} \times E_{rec}(x',y',z')\big|_{z'=0}\,dx'dy' \qquad (10)$$

where E_{in} and ω_{in} are the electric field and the minimum beam waist of the input Gaussian beam respectively, E_{rec} is the electric field of the fundamental mode of the fiber receiver. After doing the necessary coordinate transformations and evaluating the integration to get the following expression for the coupling coefficient

$$\eta = \frac{16}{\omega_{rec}^2\,\omega_{in}^2(z_{off})}$$

$$\times\exp\left\{-j\left[kz_{off} - \tan^{-1}\left(\frac{z}{z_0}\right)\right]\right\}$$

$$\times\exp\left\{-y_{off}^2\left[\frac{1}{\omega_{in}^2(z_{off})} + j\,\frac{k}{2R_{in}(z_{off})}\right]\right\} \qquad (11)$$

$$\times\left\{\frac{1}{\sqrt{4a_x a_y - c_{xy}^2}}\exp\left[\frac{b_x^2}{4a_x} + \frac{\left[2a_x b_y - cb_x\right]^2}{4a_x(4a_x a_y - c^2)}\right]\right\}$$

$$\times\left\{\frac{1}{4a_x a_y - c_{xy}^2}\exp\left[\frac{b_x^2}{4a_x} + \frac{\left[2a_x b_y - cb_x\right]^2}{4a_x(4a_x a_y - c^2)}\right]\right\}^*$$

where

$$a_x = \frac{1}{\omega_{rec}^2} + \left[j\,\frac{k}{2R_{in}(z_{off})} + \frac{1}{\omega_{in}^2(z_{off})}\right]\cos^2(\theta_y)$$

$$b_x = jk\,\sin(\theta_y)$$

$$a_y = \frac{1}{\omega_{rec}^2} + \left[j\,\frac{k}{2R_{in}(z_{off})} + \frac{1}{\omega_{in}^2(z_{off})}\right]\left[\sin^2(\theta_x)\sin^2(\theta_y) + \cos^2(\theta_x)\right]$$

$$b_y = jk\,\sin(\theta_x)\cos(\theta_y) + 2\left[j\,\frac{k}{2R(z_{off})} + \frac{1}{\omega_{in}^2(z_{off})}\right]y_{off}\,\cos(\theta_x)$$

$$c_{xy} = 2\left[j\,\frac{k}{2R(z_{off})} + + \frac{1}{\omega_{in}^2(z_{off})}\right]\sin(\theta_x)\sin(\theta_y)\cos(\theta_y)$$

$$(12)$$